Changes in Fe Oxidation Rate in Hydrothermal Plumes as a Potential Driver of Enhanced Hydrothermal Input to Near-Ridge Sediments During Glacial Terminations

J.T. Cullen and L.A. Coogan

2017

This article was originally published at:
https://doi.org/10.1002/2017GL074609

AGU PUBLICATIONS

Geophysical Research Letters

RESEARCH LETTER
10.1002/2017GL074609

Key Points:
- Reorganizations of ocean bottom water chemistry are required to explain glacial-interglacial changes in atmospheric CO_2 recorded in ice cores
- Estimated changes in bottom water O_2 and pH suggest several fold faster Fe(II) oxidation rates in the East Pacific Rise hydrothermal vent plume during the last glacial transition
- Increases in the hydrothermal component in near-ridge sediments during glacial transitions could be explained by invariant hydrothermal vent fluxes into ocean bottom water that changed in O_2 content and pH across these transitions

Supporting Information:
- Supporting Information S1

Correspondence to:
J. T. Cullen,
jcullen@uvic.ca

Citation:
Cullen, J. T., & Coogan, L. A. (2017). Changes in Fe oxidation rate in hydrothermal plumes as a potential driver of enhanced hydrothermal input to near-ridge sediments during glacial terminations. *Geophysical Research Letters*, *44*, 11,951–11,958. https://doi.org/10.1002/2017GL074609

Received 19 JUN 2017
Accepted 27 NOV 2017
Accepted article online 4 DEC 2017
Published online 14 DEC 2017

Changes in Fe Oxidation Rate in Hydrothermal Plumes as a Potential Driver of Enhanced Hydrothermal Input to Near-Ridge Sediments During Glacial Terminations

J. T. Cullen[1] and **L. A. Coogan**[1]

[1]School of Earth and Ocean Sciences, University of Victoria, Victoria, British Columbia, Canada

Abstract Recent studies have hypothesized that changes in sea level due to glacial-interglacial cycles lead to changes in the rate of melt addition to the crust at mid-ocean ridges with globally significant consequences. Arguably the most compelling evidence for this comes from increases in the hydrothermal component in near-ridge sediments during glacial-interglacial transitions. Here we explore the hypothesis that changes in ocean bottom water [O_2] and pH across glacial-interglacial transitions would lead to changes in the rate of Fe oxidation in hydrothermal plumes. A simple model shows that a several fold increase in the rate of Fe oxidation is expected at glacial-interglacial transitions. Uncertainty in bottom water chemistry and the relationship between oxidation and sedimentation rates prevent direct comparison of the model and data. However, it appears that the null hypothesis of invariant hydrothermal vent fluxes into ocean bottom water that changed in O_2 content and pH across these transitions cannot currently be discounted.

1. Introduction

Understanding the feedbacks in the earth system that operated during the Pleistocene glacial-interglacial cycles is a major challenge of the Earth sciences. Building on the idea that deglaciation induced enhanced decompression melting beneath Iceland (Hardarson & Fitton, 1991; Jull & McKenzie, 1996), Lund and Asimow (2011) hypothesized that linkages could exist between magmatic and hydrothermal processes at mid-ocean ridges and glacial-interglacial cycles. They showed that changes in pressure in the mantle, due to glacial-interglacial sea level changes, could induce small but significant (<10% at fast-spreading ridges) changes in the rate of melt production beneath mid-ocean ridges (cf. Huybers & Langmuir, 2009). While noting that numerous uncertainties exist in translating these melting anomalies into observables (e.g., melt extraction efficiency and velocity, magma chamber damping of the signal, and geometry of the melt supply region), they suggested a number of ways such signals might be found. Subsequent models of melting and melt extraction at mid-ocean ridges have also been used to predicted variations in CO_2 degassing (Burley & Katz, 2015) and ocean crust thickness, of hundreds of meters (Crowley et al., 2015a), due to the changes in pressure generated by glacial-interglacial sea level change. Comparison of such models with seafloor bathymetry has been used to argue that abyssal hill morphology is consistent with such changes in crustal thickness on Milankovitch timescales (Crowley et al., 2015a, 2015b; Huybers et al., 2016; Tolstoy, 2015, 2016). However, this model is controversial because geological processes, such as faulting, finite magma chamber mass and residence time, and lava ponding, will both create seafloor topography and damp variations in seafloor topography that would be caused by variable melt supply (e.g., Goff, 2015; Lund & Asimow, 2011; Olive et al., 2015, 2016a, 2016b).

Arguably the most compelling link between mid-ocean ridge processes and glacial-interglacial cycles comes from the covariation of the hydrothermal component of near-ridge sediments and glacial-interglacial cycles (Lund et al., 2016; Lund & Asimow, 2011; Middleton et al., 2016). In particular, Lund et al. (2016) demonstrate a clear, regional-scale, peak in the Fe, Mn, and As accumulation rate of sediments on either side of the East Pacific Rise (EPR) that occurs at the same depth in the sediment as the ~10–20 kyr decrease in planktonic calcite $\delta^{18}O$ (i.e., broadly coincident with the last deglaciation). Additionally, in one pair of cores (east and west flank) they find the same features for Termination II (~130 kyr). Lund et al. (2016) interpret the higher Fe, Mn, and As in near-ridge sediments that occur in sediments deposited during glacial terminations as indicating anomalous mantle melting during the preceding glacial maxima due to the relatively lower pressure

on the melting column during this sea level low stand. If correct, this could be associated with increased volcanic degassing of CO_2 during the glacial maximum, potentially providing a negative feedback on global cooling (Lund & Asimow, 2011; Lund et al., 2016). Alternatively, enhanced CO_2 degassing could be delayed dependent on the rate of melt transport from the base of the melting column to the surface (Burley & Katz, 2015; Huybers & Langmuir, 2017). Likewise, Middleton et al. (2016) suggest that a local peak in sedimentary Fe and Cu adjacent to the MIR vents on the Mid-Atlantic Ridge (MAR), which coincides with the last glacial maximum, reflects enhanced hydrothermal Fe input into the ocean that they hypothesize could have led to global-scale Fe fertilization. A robust understanding of the observed correlation of near-ridge sediment "hydrothermal-component" accumulation rate and glacial-interglacial cycles is clearly of broad importance.

Despite the compelling observations just discussed, some aspects of the link between peaks in hydrothermal sediment accumulation and glacial-interglacial cycles are difficult to understand. First, the fluctuations in melt supply to the crust are unlikely to exceed 10% of the steady state at fast spreading ridges but the hydrothermal sediment accumulation rate on the flanks of the EPR varied by factors of 2 to 3.5 (Lund et al., 2016). Second, during the last two deglaciations, for which Lund et al. (2016) report changes in the hydrothermal component in near-axis sediments, sea level dropped relatively slowly (although erratically) and then rose rapidly. This might be expected to lead to a slow increase in the rate of melt production followed by a rapid decrease in melt production with melt addition to the crust lagging melt generation (Crowley et al., 2015a; Lund & Asimow, 2011). Indeed, using a sophisticated model of melt production and extraction at mid-ocean ridges, Crowley et al. (2015a) suggest that at fast-spreading ridges the last two glacial terminations were associated with significant drops in melt addition to the crust that were far larger than any preceding increase in melt delivery (their Figure 1). However, the accumulation rate of the hydrothermal component in near-axis sediments appears to have been close to constant throughout most of the last 150 kyr with peaks during glacial terminations. This suggests that the process linking glacial terminations and larger amounts of a hydrothermal component in near-axis sediments may be more complex than simply reflecting the rate of melt supply to the crust. Perhaps this should not be surprising. The accumulation of elements leached from newly formed oceanic crust, or scavenged onto hydrothermal particulates (as is the case for much of the As), is not simply dependent on the supply of mantle-derived melts. Instead it depends on physical and chemical processes operating both within the crust and within the overlying water column. Here we explore one such process, which is known from the modern ocean to be important, the variation in the rate of Fe oxidation dependent on the chemical composition of the abyssal ocean. We show that changes in the bottom water that hydrothermal fluids vent into over glacial-interglacial cycles are predicted to lead to changes in Fe oxidation rate and hence the accumulation rate of hydrothermal sediments.

2. Fe Oxidation in Hydrothermal Plumes

Hydrothermal plumes at mid-ocean ridges represent important source and sink terms in the geochemical budgets of numerous trace elements in the ocean (Horner et al., 2015; Nishioka et al., 2013; Resing et al., 2015; Roshan et al., 2016; Saito et al., 2013; Tagliabue et al., 2010; Yucel et al., 2011). High-temperature, acidic, hydrothermal fluids venting at mid-ocean ridges rise rapidly into the overlying water column mixing with the surrounding bottom water, becoming diluted, cooler, and increasing in pH. Typically ~200 m from the seafloor, at dilution factors of ~1:10,000, the hydrothermal plume is neutrally buoyant and spreads laterally (e.g., German & Seyfried, 2014). Some components of the vent fluid are highly soluble and are mixed into the ocean, but others are precipitated and some constituents are scavenged from seawater onto the particulates formed leading to a net sink of these components from the ocean. Here we focus on Fe as the most important example of an element that is strongly precipitated into hydrothermal sediments.

Both complexation with organic ligands and the formation of nanoparticulate Fe through complexation with sulfide inhibit Fe oxidation, prevent precipitation, and contribute to the long-range (>4,000 km) transport of dissolved Fe away from hydrothermal vents (Resing et al., 2015; Yucel et al., 2011). Linear correlations of dissolved Fe with excess ^{3}He at midwater depths off the Southeast Pacific Rise suggest that dissolved Fe behaves conservatively with decreasing concentrations being attributable to mixing and dilution of the neutrally buoyant plume alone. However, measurements by Resing et al. (2015) and more recently published data from the same research cruise demonstrate that this complexed Fe is a very small fraction of the total Fe(II) released from vents (Fitzsimmons et al., 2017). The vast majority of Fe in the plume is lost from the dissolved

phase as it rapidly oxidizes to particulate Fe close to the ridge axis (<100 km). Indeed, according to these studies, >90% of particulate Fe (which is ~80% of the total Fe in the near field) is lost from the plume within 200 km of the ridge axis. While sparse data close to the SEPR ridge axis precluded a strict quantitative assessment of particulate Fe removal from the plume, there is a significant deviation from linearity in first-order kinetic fits using ^{3}He as a conservative tracer suggesting that near (<100 km) the ridge axis, second-order self-collision aggregative mechanisms for particulate Fe might dominate removal (Fitzsimmons et al., 2017) (supporting information). To a first approximation, the oxidation rate of Fe(II) should control particulate Fe concentrations and their aggregation and removal from the plume to the sediments within ~100 km of the ridge axis.

The oxidative half-life and residence time of Fe(II) in the plume is known to depend primarily on the redox conditions and pH prevailing in local bottom waters (Field & Sherrell, 2000; Statham et al., 2005). Seawater Fe(II) oxidation rates are described by a pseudo-first-order rate constant, k_1 (see supporting information for detailed explanation of calculations):

$$-\frac{d[Fe(II)]}{dt} = k_1[Fe(II)] \quad (1)$$

with an overall rate constant that is second order with respect to seawater pH and dependent on dissolved O_2, temperature, and salinity (Millero et al., 1987):

$$-\frac{d[Fe(II)]}{dt} = k[Fe(II)][O_2][OH^-]^2 \quad (2)$$

Recently ventilated North Atlantic waters are relatively high in pH and [O_2] compared to older deep Pacific waters as respiration of organic matter consumes O_2 and produces acids along the path of deep water circulation. A consequence of the pH-O_2 gradient in contemporary deep ocean waters is that the observed and calculated Fe(II) oxidation half-life in near-field hydrothermal plumes varies ~25-fold. At North Atlantic vents the half-life of Fe(II) can be as short as 17 min, with longer times of 2.3 h and 7.4 h at Indian Ocean and North Pacific sites respectively as pH and [O_2] decrease (Field & Sherrell, 2000; Statham et al., 2005). Could changes in deep water [O_2], T, S, and especially pH during the transition from glacial to interglacial have led to significant changes in the oxidation rate of Fe(II) and the precipitation of Fe oxides in near ridge hydrothermal sediment?

3. Changes in Bottom Water Chemistry as a Driver of Changing Hydrothermal Sediment Accumulation Rate

Reorganizations of deep ocean chemistry, affecting parameters relevant to Fe(II) oxidation, are thought to be necessary to explain the ~80 ppm changes in atmospheric CO_2 that accompany glacial-interglacial transitions (Archer et al., 2000; Broecker & Denton, 1989, 1990; Galbraith & Jaccard, 2015). Although the exact mechanism(s) by which these changes were realized remains contentious, variations in high-latitude ocean primary production, and ocean circulation and stratification are generally thought to be key. Changes in deep water temperature, salinity, [O_2], and pH must accompany this transition and will have a direct impact on the oxidation rate of reduced metals like Fe(II) at mid-ocean ridges. Here we consider these changes near to the EPR (~0–10°S, 100–110°W) hydrothermal vents studied by Lund et al. (2016) during the last glacial-interglacial transition (Table 1). Shallow-infaunal benthic foraminifera Mg/Ca paleothermometry suggests that during the Last Glacial Maximum (LGM; ~20 kya) the deep water was approximately −1.1 ± 0.3°C or 2–3°C colder than during the Holocene (Elderfield et al., 2010). A ~115 m drop in sea level would increase salinity ~3% (1 psu) in deep water which has a trivial impact on Fe oxidation rates. Benthic oxygen proxies suggest the bottom water [O_2] was ~70 μmol kg^{-1} lower at EPR vent fields during the LGM or 35–50 μmol kg^{-1} compared to ~110 μmol kg^{-1} during the Holocene (Galbraith & Jaccard, 2015). Boron isotope fractionation in benthic foraminifera supports a pH in the LGM eastern equatorial Pacific that was 0.3 ± 0.1 units higher than the Holocene (Sanyal et al., 1995, 1997). In contrast, combined Indo-Pacific sediment core foraminiferal B/Ca proxy records suggest that the vertical concentration distribution of the carbonate ion ([CO_3^{2-}]) for the LGM was very similar to that observed for the Holocene (Allen et al., 2015; Yu et al., 2013) despite authigenic uranium and opal flux evidence for higher deep water dissolved inorganic carbon (DIC) during the LGM (Jaccard et al., 2009, 2014). Apparent oxygen utilization (313 μmol kg^{-1}) calculated from LGM T

Geophysical Research Letters

10.1002/2017GL074609

Table 1
Parameters Used to Calculate Fe(II) Oxidation Rate in Ambient Seawater at the East Pacific Rise Over the Last Glacial Termination

									Fe(II) oxidation rate					Fe(II) half-life			
Depth	Temperature (°C)	Salinity[a]	O_2 (μmol kg^{-1})[b]	pH_{sws}[c]	pK_w[d]	pOH[e]	log k[f]	k_1 (min^{-1})[f]	Mean	Range	SD	Normalized to Holocene rate	SD	Hour	Mean	Range	SD
Holocene[g]																	
2372	1.92	34.661	104	7.748	14.122	6.374	14.248	0.0033	0.0035	0.0003	0.0002	1.00	0.07	3.52	3.35	0.34	0.24
2570	1.84	34.666	110	7.755	14.119	6.364	14.246	0.0036						3.18			
Transitition																	
-	0.5	35.2	104	8.348	14.187	5.839	14.219	0.0361	0.0237	0.0304	0.016	6.84	4.74	0.32	0.76	0.98	0.53
-	0.5	35.2	104	8.048	14.187	6.139	14.219	0.0091						1.27			
-	0.5	35.2	110	8.348	14.180	5.832	14.219	0.0395						0.29			
-	0.5	35.2	110	8.048	14.180	6.132	14.219	0.0099						1.16			
Last Glacial Maximum																	
-	−1.1	35.7	35	8.148	14.262	6.114	14.176	0.0031	0.0017	0.0041	0.0015	0.48	0.43	3.72	12.12	19.59	7.79
-	−1.1	35.7	35	8.148	14.262	6.114	14.176	0.0012						9.34			
-	−1.1	35.7	50	7.948	14.255	6.307	14.176	0.0046						2.52			
-	−1.1	35.7	50	7.948	14.255	6.307	14.176	0.0018						6.32			
-	−1.1	35.7	35	7.761	14.262	6.501	14.176	0.0005						22.10			
-	−1.1	35.7	35	7.754	14.262	6.508	14.176	0.0005						22.06			
-	−1.1	35.7	50	7.761	14.255	6.494	14.176	0.0007						15.47			
-	−1.1	35.7	50	7.754	14.255	6.501	14.176	0.0007						15.44			

[a]Sanyal et al. (1997). [b]LGM and Transition oxygen from Galbraith and Jaccard (2015). [c]pH values taken from Sanyal et al. (1995, 1997) or calculated from DIC and [CO_3^{2-}] from Allen et al. (LGM, Yu et al., 2013; Marchitto et al., 2005 Transition, and Field & Sherrell, 2000 Holocene). [d]Calculated after Millero (1995) using T and S and corrected for pressure. [e]pOH = pK_w – pH. [f]Calculated after Millero et al. (1987) after applying a correction for pH and pK_w to express them on the free proton scale. [g]Depth, T, S, O_2, and pH from Field and Sherrell (2000).

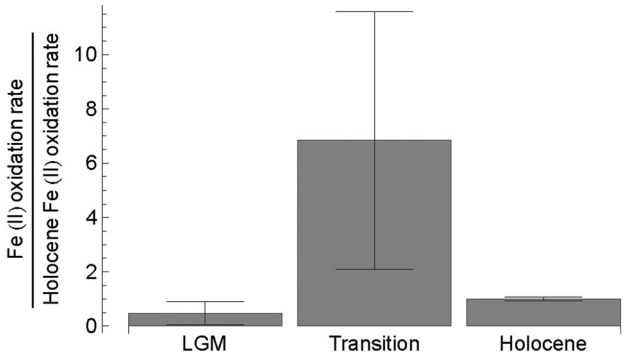

Figure 1. Calculated Fe(II) oxidation rates normalized to Holocene rates (Field & Sherrell, 2000) for bottom water conditions estimated during the LGM, transition, and early Holocene at the EPR vent system at ~10°N, 110°W. Oxidation rates were calculated after Millero et al. (1987) using information provided in Table 1.

and S and $[O_2]$ = 35–50 μmol kg^{-1} can be used to estimate the amount of additional respired carbon (+216 μmol kg^{-1}) and total DIC (~2,577–2,579 μmol kg^{-1}) in the deep water during the LGM assuming "Redfield" stoichiometry ($DIC/[O_2]$ = 117/170) (Anderson & Sarmiento, 1994). Given that LGM $[CO_3^{2-}]$ was similar to the Holocene, we can therefore constrain LGM deep water pH to a range of 7.75–7.76. We use both estimates of pH to calculate Fe oxidation kinetics to provide a conservative accounting of uncertainty in rates for the LGM.

The LGM to Holocene transition in ocean chemistry has been proposed to be driven by diminished ocean productivity at high latitudes, increased ventilation of the high latitude Southern Ocean and shoaling of remineralization horizons in the Pacific (Galbraith & Jaccard, 2015). These changes appear to have occurred early in the deglaciation (~17.5 to ~14 ka) and best explain observations of diminished pools of respired carbon in the deep ocean, increased deep ocean oxygenation and an increased pool of unutilized NO_3^- in Southern Ocean surface waters (François et al., 1997; Galbraith & Jaccard, 2015; Sigman & Boyle, 2000). To calculate Fe(II) oxidation rates during the deglaciation, we assume that T and S, which are less significant factors with respect to Fe(II) rates, changed gradually with intermediate values during the transition. Dissolved $[O_2]$ at the EPR would have changed on the timescale of ocean circulation as ventilation changes in the Southern Ocean and diminished demand for respiration propagated through deep water. In contrast, modeling and proxy based reconstructions of carbonate ion concentrations $[CO_3^{2-}]$ in the deep Pacific during the transition suggest that the release of carbon from these waters and the delayed process of carbonate compensation would result in $[CO_3^{2-}]$, and pH, peaks (Allen et al., 2015; Boyle, 1988a, 1988b; Marchitto et al., 2005; Yu et al., 2013). Increases of $[CO_3^{2-}]$ reconstructed from B/Ca, Cd/Ca, and Zn/Cd in benthic foraminifera suggest positive $\Delta[CO_3^{2-}]$ of ~10–30 μmol kg^{-1} during the transition which, assuming constant alkalinity during the transition, represents a corresponding +ΔpH of ~0.1–0.2 units given typical ranges of ALK and DIC in the Pacific. Given this, we estimate that $[O_2]$ would be similar to Holocene values while pH would have increased ~0.1–0.2 units relative to LGM values during the transition before falling to Holocene values as ocean alkalinity decreased in response to lower DIC at depth.

Based on the changes in ocean chemistry outlined above, the oxidative half-life of Fe in hydrothermal plumes along the EPR can be determined (equations (1) and (2)). While there is uncertainty in the parameter estimates a roughly sevenfold increase in Fe oxidation rate is predicted (Figure 1) with the pH change playing the dominant role. This is similar to the observed changes in Fe accumulation rates reported (2-fold to 3.5-fold; Lund et al., 2016) and much larger than the expected change in rate of melt production due to sea level fall at the end of the last glaciation. Thus, while there are uncertainties in both the time evolution of the composition of the seawater above the EPR and the link between oxidation rate and sedimentation rate, it seems clear that changes in bottom water chemistry need to be accounted for if accumulation rates of hydrothermal sediments are to be correctly interpreted. The associated peak in As content of the sediments is simply a tracer of the Fe oxyhydroxide content of the sediments as As is largely scavenged from seawater onto particulate Fe. In contrast, Mangini et al. (1990) proposed that enhanced Mn nodule growth rates, and sedimentary Mn accumulation rates, at Termination 1 were not due to changing hydrothermal input but instead reflect changing bottom water conditions. In their model, Mn was released from seafloor sediments into the ocean during glacial periods, due to low bottom water O_2 levels, followed by redeposition of this Mn due to increased bottom water O_2 during the transition (Mangini et al., 1990). This model predicts increased Mn accumulation at the same time as our model predicts increased Fe accumulation because both are driven by changing bottom water conditions even though the metals have different origins. If there were changes in hydrothermal flux across glacial-interglacial transitions quantifying the magnitude of this from sediment cores will require a comprehensive understanding of processes operating in the overlying water column. Furthermore, irrespective of whether there were changes in the hydrothermal flux across glacial-interglacial transitions, the dispersal of hydrothermal Fe is predicted to have changed due to changing bottom water conditions.

4. Summary

Recent models have suggested a link between glacial-interglacial cycles of sea level change and melt production at mid-ocean ridges (Burley & Katz, 2015; Crowley et al., 2015a; Huybers & Langmuir, 2009, 2017; Lund & Asimow, 2011; Lund et al., 2016; Tolstoy, 2015). Arguably the strongest support for this model comes from the remarkable coherence of changes in hydrothermal sediment accumulation on both sides of the EPR, across multiple sampling sites, that closely match in time the transition from glacial to interglacial (Lund et al., 2016). Here we caution that such a signal is expected, even if the hydrothermal vent flux remained constant, due to changes in bottom water chemistry leading to increased Fe oxidation rate in the hydrothermal plume during this transition. Other processes, such as changes in diagenetic modification of the sediments (e.g., Mills et al., 2010), will also need considering if a changes in hydrothermal flux is to be fully quantified from sediment records. The model proposed here could be tested using sediment cores from different places along the global ridge system where the timing and magnitude of changes in bottom water chemistry across glacial-interglacial transitions differ. However, the inherently episodic nature of magmatism at slow-spreading ridges will complicate the signature in these settings. For example, Middleton et al. (2016) report a peak in hydrothermal sediment accumulation rate coincident with the last glacial termination on the Mid-Atlantic ridge that at first sight may appear inconsistent with our model given the difference in deep water conditions in the Atlantic than Pacific at this time. However, this sediment core comes from within a vent field and hence does not integrate hydrothermal activity along a broad length of the ridge but instead likely reflects the well-known episodic magmatism at slow-spreading ridges. Cores from off axis along the intermediate spreading rate Juan de Fuca ridge, in the North Pacific, would be useful in testing the model proposed here.

Acknowledgments
We thank two anonymous reviewers and James Rae, William Seyfried, Bob Anderson, Samuel Jaccard and Eric Galbraith for discussions which improved the manuscript. Equations and data used in the calculations presented in the manuscript are available in Table 1 and the supporting information. J. T. C. and L. A. C. were supported by the Natural Sciences and Engineering Research Council of Canada.

References

Allen, K. A., Sikes, E. L., Hönisch, B., Elmore, A. C., Guilderson, T. P., Rosenthal, Y., & Anderson, R. F. (2015). Southwest Pacific deep water carbonate chemistry linked to high southern latitude climate and atmospheric CO_2 during the Last Glacial Termination. *Quaternary Science Reviews*, *122*, 180–191. https://doi.org/10.1016/j.quascirev.2015.05.007

Anderson, L. A., & Sarmiento, J. L. (1994). Redfield ratios of remineralization determined by nutrient data analysis. *Global Biogeochemical Cycles*, *8*(1), 65–80. https://doi.org/10.1029/93GB03318

Archer, D., Winguth, A., Lea, D., & Mahowald, N. (2000). What caused the glacial/interglacial atmospheric pCO_2 cycles? *Reviews of Geophysics*, *38*(2), 159–189. https://doi.org/10.1029/1999RG000066

Barrett, T. J., Taylor, P. N., & Lugoqski, J. (1987). Metalliferous sediments from DSDP Leg 92: The East Pacific Rise transect. *Geochimica et Cosmochimica Acta*, *51*(9), 2241–2253. https://doi.org/10.1016/0016-7037(87)90278-X

Boyle, E. A. (1988a). The role of vertical chemical fractionation in controlling late quaternary atmospheric carbon-dioxide. *Journal of Geophysical Research*, *93*(C12), 15,701–15,714. https://doi.org/10.1029/JC093iC12p15701

Boyle, E. A. (1988b). Vertical ocean nutrient fractionation and glacial interglacial CO_2 cycles. *Nature*, *331*(6151), 55–56. https://doi.org/10.1038/331055a0

Broecker, W. S., & Denton, G. H. (1989). The role of ocean-atmosphere reorganizations in glacial cycles. *Geochimica et Cosmochimica Acta*, *53*(10), 2465–2501. https://doi.org/10.1016/0016-7037(89)90123-3

Broecker, W. S., & Denton, G. H. (1990). The role of ocean-atmosphere reorganizations in glacial cycles. *Quaternary Science Reviews*, *9*(4), 305–341. https://doi.org/10.1016/0277-3791(90)90026-7

Burley, J. M. A., & Katz, R. F. (2015). Variations in mid-ocean ridge CO_2 emissions driven by glacial cycles. *Earth and Planetary Science Letters*, *426*, 246–258. https://doi.org/10.1016/j.epsl.2015.06.031

Crowley, J. W., Katz, R. F., Huybers, P., Langmuir, C. H., & Park, S.-H. (2015a). Glacial cycles drive variations in the production of oceanic crust. *Science*, *347*(6227), 1237–1240. https://doi.org/10.1126/science.1261508

Crowley, J. W., Katz, R. F., Huybers, P., Langmuir, C. H., & Park, S.-H. (2015b). Response to Comment on "Glacial cycles drive variations in the production of oceanic crust". *Science*, *349*(6252), 1065–1065. https://doi.org/10.1126/science.aab3497

Elderfield, H., Greaves, M., Barker, S., Hall, I. R., Tripati, A., Ferretti, P., … Daunt, C. (2010). A record of bottom water temperature and seawater delta O-18 for the Southern Ocean over the past 440 kyr based on Mg/Ca of benthic foraminiferal Uvigerina spp. *Quaternary Science Reviews*, *29*(1-2), 160–169. https://doi.org/10.1016/j.quascirev.2009.07.013

Feely, R. A., Trefry, J. H., Massoth, G. J., & Metz, S. (1991). A comparison of the scavenging of phosphorus and arsenic from seawater by hydrothermal iron oxyhydroxides in the Atlantic and Pacific Oceans. *Deep Sea Research Part A. Oceanographic Research Papers*, *38*(6), 617–623. https://doi.org/10.1016/0198-0149(91)90001-V

Field, M. P., & Sherrell, R. M. (2000). Dissolved and particulate Fe in a hydrothermal plume at 9°45′N, East Pacific Rise: Slow Fe (II) oxidation kinetics in Pacific plumes. *Geochimica et Cosmochimica Acta*, *64*(4), 619–628. https://doi.org/10.1016/S0016-7037(99)00333-6

Fitzsimmons, J. N., John, S. G., Marsay, C. M., Hoffman, C. L., Nicholas, S. L., Toner, B. M., … Sherrell, R. M. (2017). Iron persistence in a distal hydrothermal plume supported by dissolved-particulate exchange. *Nature Geoscience*, *10*(3), 195–201. https://doi.org/10.1038/ngeo2900

François, R., Altabet, M. A., Yu, E.-F., Sigman, D. M., Bacon, M. P., Frank, M., … Labeyrie, L. D. (1997). Contribution of Southern Ocean surface-water stratification to low atmospheric CO_2 concentrations during the last glacial period. *Nature*, *289*, 929–935.

Frank, M., Eckhardt, J.-D., Eisenhauer, A., Kubik, P. W., Dittrich-Hannen, B., Segl, M., & Mangini, A. (1994). Beryllium 10, thorium 230, and protactinium 231 in Galapagos microplate sediments: Implications of hydrothermal activity and paleoproductivity changes during the last 100,000 years. *Paleoceanography*, *9*(4), 559–578. https://doi.org/10.1029/94PA01132

Galbraith, E. D., & Jaccard, S. L. (2015). Deglacial weakening of the oceanic soft tissue pump: Global constraints from sedimentary nitrogen isotopes and oxygenation proxies. *Quaternary Science Reviews*, *109*, 38–48. https://doi.org/10.1016/j.quascirev.2014.11.012

German, C. R., & Seyfried, W. E. Jr. (2014). Hydrothermal processes. In H. D. Holland, & K. B. Turekian (Eds.), *Treatise on Geochemistry* (2nd ed., pp. 191–233). Oxford: Elsevier. https://doi.org/10.1016/B978-0-08-095975-7.00607-0

Goff, J. A. (2015). Comment on "Glacial cycles drive variations in the production of oceanic crust". *Science*, *349*(6252), 1065. https://doi.org/10.1126/science.aab2350

Hardarson, B. S., & Fitton, J. G. (1991). Increased mantle melting beneath Snaefellsjokull volcano during Late Pleistocene deglaciation. *Nature*, *353*(6339), 62–64. https://doi.org/10.1038/353062a0

Horner, T. J., Williams, H. M., Hein, J. R., Saito, M. A., Burton, K. W., Halliday, A. N., & Nielsen, S. G. (2015). Persistence of deeply sourced iron in the Pacific Ocean. *Proceedings of the National Academy of Sciences of the United States of America*, *112*(5), 1292–1297. https://doi.org/10.1073/pnas.1420188112

Huybers, P., & Langmuir, C. (2009). Feedback between deglaciation, volcanism, and atmospheric CO_2. *Earth and Planetary Science Letters*, *286*(3-4), 479–491. https://doi.org/10.1016/j.epsl.2009.07.014

Huybers, P., Langmuir, C., Katz, R. F., Ferguson, D., Proistosescu, C., & Carbotte, S. (2016). Comment on "Sensitivity of seafloor bathymetry to climate-driven fluctuations in mid-ocean ridge magma supply". *Science*, *352*(6292), 1405–1405. https://doi.org/10.1126/science.aae0451

Huybers, P., & Langmuir, C. H. (2017). Delayed CO_2 emissions from mid-ocean ridge volcanism as a possible cause of late-Pleistocene glacial cycles. *Earth and Planetary Science Letters*, *457*, 238–249. https://doi.org/10.1016/j.epsl.2016.09.021

Jaccard, S., Galbraith, E., Frölicher, T., & Gruber, N. (2014). Ocean (de)oxygenation across the last deglaciation: Insights for the future. *Oceanography*, *27*(1), 26–35. https://doi.org/10.5670/oceanog.2014.05

Jaccard, S. L., Galbraith, E. D., Sigman, D. M., Haug, G. H., Francois, R., Pedersen, T. F., … Thierstein, H. R. (2009). Subarctic Pacific evidence for a glacial deepening of the oceanic respired carbon pool. *Earth and Planetary Science Letters*, *277*(1-2), 156–165. https://doi.org/10.1016/j.epsl.2008.10.017

Jull, M., & McKenzie, D. (1996). The effect of deglaciation on mantle melting beneath Iceland. *Journal of Geophysical Research*, *101*(B10), 21,815–21,828. https://doi.org/10.1029/96JB01308

Lund, D. C., & Asimow, P. D. (2011). Does sea level influence mid-ocean ridge magmatism on Milankovitch timescales? *Geochemistry, Geophysics, Geosystems*, *12*(12), Q03014. https://doi.org/10.1029/2011GC003693

Lund, D. C., Asimow, P. D., Farley, K. A., Rooney, T. O., Seeley, E., Jackson, E. W., & Durham, Z. M. (2016). Enhanced East Pacific Rise hydrothermal activity during the last two glacial terminations. *Science*, *351*(6272), 478–482. https://doi.org/10.1126/science.aad4296

Mangini, A., Eisenhauer, A., & Walter, P. (1990). Response of manganese in the ocean to the climatic cycles in the Quaternary. *Paleoceanography*, *5*(5), 811–821. https://doi.org/10.1029/PA005i005p00811

Marchitto, T. M., Lynch-Stieglitz, J., & Hemming, S. R. (2005). Deep Pacific $CaCO_3$ compensation and glacial–interglacial atmospheric CO_2. *Earth and Planetary Science Letters*, *231*(3-4), 317–336. https://doi.org/10.1016/j.epsl.2004.12.024

Middleton, J. L., Langmuir, C. H., Mukhopadhyay, S., McManus, J. F., & Mitrovica, J. X. (2016). Hydrothermal iron flux variability following rapid sea level changes. *Geophysical Research Letters*, *43*, 3848–3856. https://doi.org/10.1002/2016GL068408

Millero, F. J. (1995). Thermodynamics of the carbon dioxide system in the oceans. *Geochimica et Cosmochimica Acta*, *59*(4), 661–677. https://doi.org/10.1016/0016-7037(94)00354-O

Millero, F. J., Sotolongo, S., & Izaguirre, M. (1987). The oxidation kinetics of Fe(II) in seawater. *Geochimica et Cosmochimica Acta*, *51*(4), 793–801. https://doi.org/10.1016/0016-7037(87)90093-7

Mills, R. A., Taylor, S. L., Pälike, H., & Thomson, J. (2010). Hydrothermal sediments record changes in deep water oxygen content in the SE Pacific. *Paleoceanography*, *25*, PA422. https://doi.org/10.1029/2010PA001959

Nishioka, J., Obata, H., & Tsumune, D. (2013). Evidence of an extensive spread of hydrothermal dissolved iron in the Indian Ocean. *Earth and Planetary Science Letters*, *361*, 26–33. https://doi.org/10.1016/j.epsl.2012.11.040

Olive, J.-A., Behn, M. D., Ito, G., Buck, W. R., Escartín, J., & Howell, S. (2015). Sensitivity of seafloor bathymetry to climate-driven fluctuations in mid-ocean ridge magma supply. *Science*, *350*(6258), 310–313. https://doi.org/10.1126/science.aad0715

Olive, J.-A., Behn, M. D., Ito, G., Buck, W. R., Escartín, J., & Howell, S. (2016a). Response to Comment on "Sensitivity of seafloor bathymetry to climate-driven fluctuations in mid-ocean ridge magma supply". *Science*, *353*(6296), 229. https://doi.org/10.1126/science.aaf2022

Olive, J.-A., Behn, M. D., Ito, G., Buck, W. R., Escartin, J., & Howell, S. (2016b). Response to Comment on "Sensitivity of seafloor bathymetry to climate-driven fluctuations in mid-ocean ridge magma supply". *Science*, *352*(6292), 1405. https://doi.org/10.1126/science.aaf2021

Pester, N. J., Rough, M., Ding, K., & Seyfried, W. E. Jr. (2011). A new Fe/Mn geothermometer for hydrothermal systems: Implications for high-salinity fluids at 13°N on the East Pacific Rise. *Geochimica et Cosmochimica Acta*, *75*(24), 7881–7892. https://doi.org/10.1016/j.gca.2011.08.043

Resing, J. A., Sedwick, P. N., German, C. R., Jenkins, W. J., Moffett, J. W., Sohst, B. M., & Tagliabue, A. (2015). Basin-scale transport of hydrothermal dissolved metals across the South Pacific Ocean. *Nature*, *523*(7559), 200–203. https://doi.org/10.1038/nature14577

Roshan, S., Wu, J. F., & Jenkins, W. J. (2016). Long-range transport of hydrothermal dissolved Zn in the tropical South Pacific. *Marine Chemistry*, *183*, 25–32. https://doi.org/10.1016/j.marchem.2016.05.005

Saito, M. A., Noble, A. E., Tagliabue, A., Goepfert, T. J., Lamborg, C. H., & Jenkins, W. J. (2013). Slow-spreading submarine ridges in the South Atlantic as a significant oceanic iron source. *Nature Geoscience*, *6*(9), 775–779. https://doi.org/10.1038/ngeo1893

Sanyal, A., Hemming, N. G., Broecker, W. S., & Hanson, G. N. (1997). Changes in pH in the eastern equatorial Pacific across stage 5–6 boundary based on boron isotopes in foraminifera. *Global Biogeochemical Cycles*, *11*(1), 125–133. https://doi.org/10.1029/97GB00223

Sanyal, A., Hemming, N. G., Hanson, G. N., & Broecker, W. S. (1995). Evidence for a higher pH in the glacial ocean from boron isotopes in foraminifera. *Nature*, *373*(6511), 234–236. https://doi.org/10.1038/373234a0

Schaller, T., Morford, J., Emerson, S. R., & Feely, R. A. (2000). Oxyanions in metalliferous sediments: Tracers for paleoseawater metal concentrations? *Geochimica et Cosmochimica Acta*, *64*(13), 2243–2254. https://doi.org/10.1016/S0016-7037(99)00443-3

Sigman, D. M., & Boyle, E. A. (2000). Glacial/interglacial variations in atmospheric carbon dioxide. *Nature*, *407*(6806), 859–869. https://doi.org/10.1038/35038000

Statham, P. J., German, C. R., & Connelly, D. P. (2005). Iron(II) distribution and oxidation kinetics in hydrothermal plumes at the Kairei and Edmond vent sites, Indian Ocean. *Earth and Planetary Science Letters*, *236*(3-4), 588–596. https://doi.org/10.1016/j.epsl.2005.03.008

Tagliabue, A., Bopp, L., Dutay, J.-C., Bowie, A. R., Chever, F., Jean-Baptiste, P., … Jeandel, C. (2010). Hydrothermal contribution to the oceanic dissolved iron inventory. *Nature Geoscience*, *3*(4), 252–256. https://doi.org/10.1038/ngeo818

Tolstoy, M. (2015). Mid-ocean ridge eruptions as a climate valve. *Geophysical Research Letters*, *42*, 1346–1351. https://doi.org/10.1002/2014GL063015

Tolstoy, M. (2016). Comment on "Sensitivity of seafloor bathymetry to climate-driven fluctuations in mid-ocean ridge magma supply". *Science*, *353*(6296), 229. https://doi.org/10.1126/science.aaf0625

Yu, J. M., Anderson, R. F., Jin, Z. D., Rae, J. W. B., Opdyke, B. N., & Eggins, S. M. (2013). Responses of the deep ocean carbonate system to carbon reorganization during the Last Glacial-interglacial cycle. *Quaternary Science Reviews*, *76*, 39–52. https://doi.org/10.1016/j.quascirev.2013.06.020

Yucel, M., Gartman, A., Chan, C. S., & Luther, G. W. (2011). Hydrothermal vents as a kinetically stable source of iron-sulphide-bearing nanoparticles to the ocean. *Nature Geoscience*, *4*(6), 367–371. https://doi.org/10.1038/ngeo1148